Research Article

Received: 17 September 2025 Revised: 11 November 2025 Published online in Wiley Online Library:

(wileyonlinelibrary.com) DOI 10.1002/ps.70462

Novel cinnamic acid-ribavirin conjugates: design, synthesis, antiviral activity against tobacco mosaic virus and mechanistic study

Min Luo,[a] Chen Chen,[a] Min Xu,[a] Wen-Xin Lv[a*] and Yonggui Robin Chi[a,b*]

Abstract

BACKGROUND: Plant viral diseases represent a serious threat to global agricultural productivity and sustainable development. Most commercially available antiviral agents function primarily as protectants. However, the long-term and repetitive application of conventional broad-spectrum antiviral agents has led to the emergence of resistance, diminishing their field efficacy. To discover new antiviral drugs, we designed and synthesized 31 novel ribavirin derivatives incorporating cinnamic acid motifs *via* a lead optimization strategy and evaluated their anti-tobacco mosaic virus (TMV) activity.

RESULTS: Biological assays revealed that compound A23 **exhibited potent protective activity against TMV, with an EC_{50} of 131.1 μg/mL, which was significantly lower than that of ribavirin (529.9 μg/mL) and ningnanmycin (248.4 μg/mL). Further research indicated that compound** A23 **significantly enhanced the activity of defense-related enzymes and regulated the plant hormone signal transduction pathway as well as the plant-pathogen interaction pathway in tobacco plants. Notably, it upregulated the expression of key genes *NPR1* and *PR-1* in the salicylic acid (SA) signaling pathway, thereby effectively enhancing the plant's defense response and resistance against TMV.**

CONCLUSION: These results demonstrate that compound A23 **possesses remarkable bioactivity and effectively controls TMV infection by inducing host plant immunity. Its promising efficacy supports its potential as a candidate agent for controlling plant viral diseases and warrants further investigation.**

Supporting information may be found in the online version of this article.

Keywords: lead optimization; antiviral activity; TMV; mechanisms; defense enzymes; transcriptomics analysis

1 INTRODUCTION

Plant viral diseases impose severe and persistent threats to global agricultural productivity and crop quality, leading to substantial annual economic losses estimated to reach hundreds of millions of dollars worldwide.[1–4] Tobacco mosaic virus (TMV) remains one of the most intractable plant viral pathogens worldwide, characterized by its exceptionally broad host range and extraordinary environmental persistence. It successfully infects more than 885 species across 65 plant genera and severely impacts numerous economically important crops, including cucumber, tobacco, tomato, and peppers.[5–7] Chemical intervention remains a primary strategy for controlling TMV infections. However, current antiviral agents are largely unsatisfactory due to their limited control effect, photothermal instability and a propensity to elicit resistance. For instance, two commercial antiviral agents used against plant virus diseases, ningnanmycin (NNM) and ribavirin, have significant but distinct limitations. NNM is limited by its poor environmental stability, making it prone to decomposition, whereas the primary drawback of ribavirin is its limited efficacy against a broad spectrum of viruses.[8–10] To address these persistent challenges, the development of novel antiviral compounds with innovative mechanisms of action, high target selectivity, and improved environmental compatibility has become a critical research priority within agricultural chemistry and plant protection science.

In the development of antiviral agents, nucleoside analogues represent an important source of lead compounds (Fig. 1(A)). These compounds structurally mimic natural nucleosides and exert broad-spectrum antiviral activity by competitively inhibiting viral genome replication through targeting viral RNA-dependent RNA polymerase. Many successful antiviral agents have been developed through the systematic structural optimization of nucleoside analogues.[11] Ribavirin, as a representative nucleoside analogue, has been used in human medicine for the control of respiratory syncytial virus, hepatitis virus, and influenza virus.[12,13] Its successful application has also provided insights for plant virus

* *Correspondence to: W-X Lv and YR Chi, State Key Laboratory of Green Pesticide; Center for R&D of Fine Chemicals of Guizhou University, Guiyang, 550025, China. E-mail: wxlv@gzu.edu.cn; robinchi@ntu.edu.sg*

a *State Key Laboratory of Green Pesticide, Center for R&D of Fine Chemicals of Guizhou University, Guiyang, China*

b *School of Chemistry, Chemical Engineering, and Biotechnology, Nanyang Technological University, Singapore, Singapore*

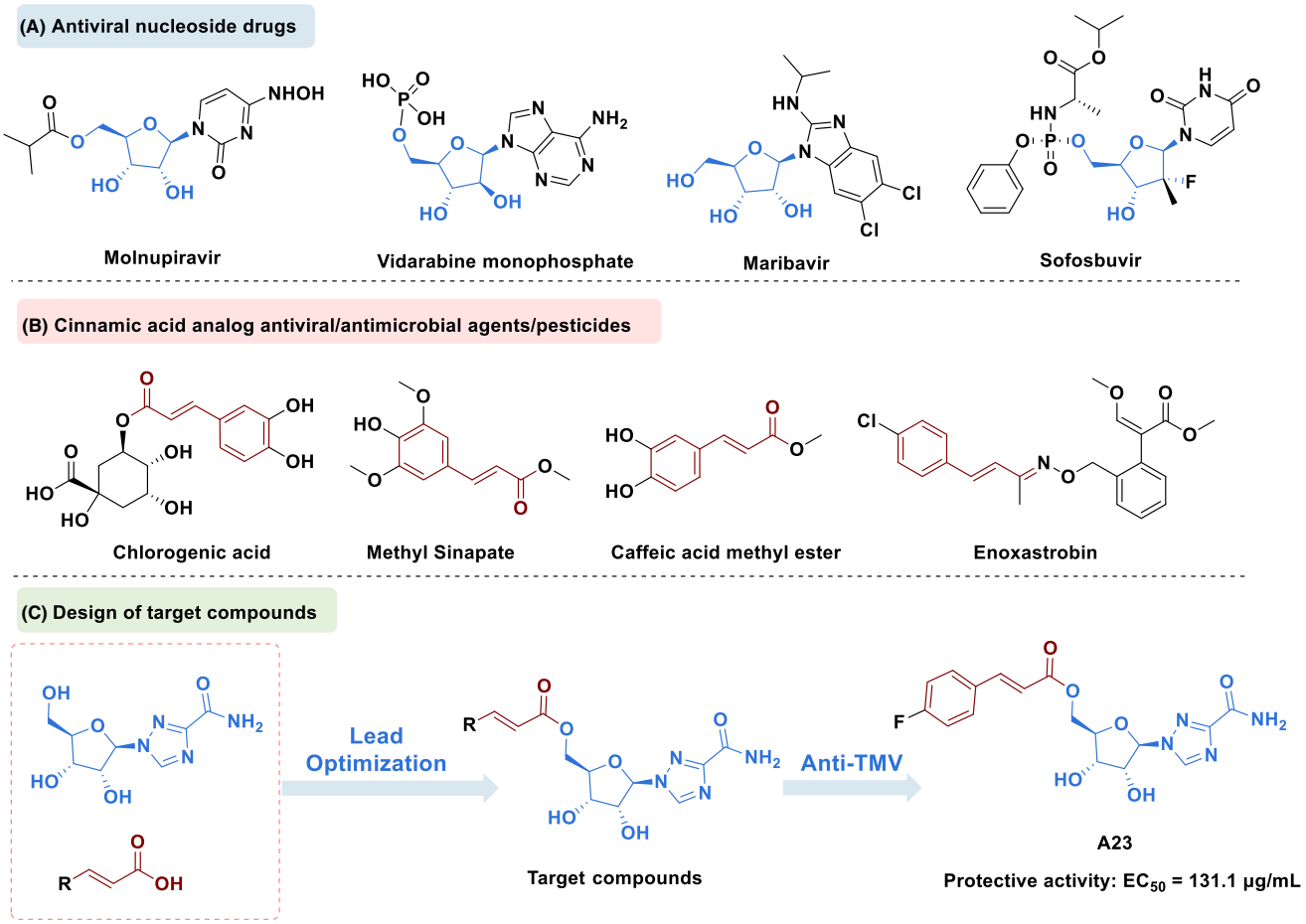

Figure 1. Design of target compounds.

management. Studies have shown that ribavirin exhibits varying degrees of protective and therapeutic activity against multiple plant viruses, such as TMV, Potato virus X (PVX), and Cucumber mosaic virus (CMV).[14] In recent years, it has been further demonstrated to inhibit Tomato spotted wilt virus (TSWV) replication, and structural biology approaches have revealed its dual-target inhibitory mechanism by binding to the active site of the viral polymerase.[15] Nevertheless, ribavirin still suffers from issues such as the potential to induce drug resistance. Therefore, ongoing research continues to focus on structural optimization and mechanistic studies of this compound.

Meanwhile, natural products have become important resources for developing green pesticides owing to their structural diversity, low environmental impact, and potential to activate the plant immune system.[16,17] We focused on cinnamic acid and its derivatives—such as *P*-coumaric, sinapic, and ferulic acids—which are not only widely distributed in plants and serve as key intermediates in the phenylpropanoid pathway,[18,19] but more importantly, function as precursors for salicylic acid (SA) biosynthesis and participate in systemic acquired resistance (SAR) signaling. Furthermore, these compounds can directly inhibit pathogen growth or replication, exhibiting broad-spectrum biological activities such as antifungal,[20,21] antibacterial,[22] insecticidal,[23] herbicidal,[24] and antiviral effects[25,26] (Fig. 1(B)). Notably, the biosynthesis pathway of salicylic acid (SA)—a central phytohormone in plant defense—has been recently elucidated in depth.[27] This discovery provides a molecular basis for our rationale for using these SA precursors to design immune-priming-based antiviral strategies. This approach is consistent with our subsequent finding that the antiviral activity of these compounds may be linked to the potentiation of SA-mediated defense pathways.

In our group's previous work,[28] nucleoside ester derivatives demonstrated moderate antiviral activity and served as promising scaffolds for antiviral agent development. Herein, using ribavirin as the lead compound, this study designed and synthesized a series of novel cinnamic acid-conjugated ribavirin derivatives through structural modification (Fig. 1(C)). Their anti-TMV activity was evaluated using the half-leaf local lesion assay. Biological assays showed that some derivatives displayed significant antiviral properties, with compound **A23** exhibiting the most potent *in vivo* antiviral protective activity, outperforming commonly used reference compounds ribavirin and NNM. Furthermore, preliminary mechanistic investigations of **A23** were performed using transcriptomic analysis, TMV-GFP systemic infection assays, defensive enzyme activity, and determination of chlorophyll content tests.

2 MATERIALS AND METHODS

2.1 Chemicals and instruments

Commercially available materials purchased from Leyan (Shanghai, China), Bide (Shanghai, China) and Energy Chemistry (Anhui, China) were used directly in the experiment without

further purification. The ^{1}H, ^{19}F, and ^{13}C nuclear magnetic resonance (NMR) spectra were recorded on a Bruker Avance III 400 MHz spectrometer (Bruker BioSpin AG, Germany) in deuterated dimethyl sulfoxide-d_6 (DMSO-d_6). High-resolution mass spectrometry (HRMS) was obtained on a Thermo Fisher Q Exactive mass spectrometer (Thermo Fisher Scientific, USA). The melting points of all the compounds were measured using a WGX-4B binocular microscopic melting point apparatus (Nanjing Weiguang Instrument and Equipment Co., Ltd., China).

2.2 General procedure for the synthesis of A1 − A31

According to the reported methods,[29] intermediate **a** was prepared. A reaction mixture of intermediate **a** (0.70 mmol, 1.0 equiv.), various cinnamic acid derivatives (0.77 mmol, 1.1 equiv.), *N*,*N*-diisopropylcarbodiimide (0.77 mmol, 1.1 equiv.) and 4-dimethylaminopyridine (0.017 mmol, 0.024 equiv.) in CH_2Cl_2 (8 mL) was stirred at room temperature for 2–6 h. The mixture was then washed with saturated brine and extracted with CH_2Cl_2 (3 × 20 mL). The combined organic layers were dried over anhydrous Na_2SO_4 and concentrated under reduced pressure. The resulting residue was purified by column chromatography using CH_2Cl_2/MeOH (100:1 to 100:2, v/v) to obtain intermediates **b1–b31**. To a solution of compounds **b1–b31** in anhydrous methanol (6 mL) was added concentrated hydrochloric acid (0.3 mL), and the reaction was stirred at room temperature for 8 h. After removal of the solvent under reduced pressure, the crude product was purified by column chromatography using CH_2Cl_2/MeOH (100:1 to 100:5, v/v) to afford target compounds **A1–A31**. The synthetic route is shown in Fig. 2. The physical properties, ^{1}H NMR, ^{13}C NMR, ^{19}F NMR, and HRMS data of the synthesized compounds can be found in Supporting Information 1.

2.3 Antiviral bioassay against TMV

Nicotiana tabacum cv. K326 plants were systemically infected with TMV for over 3 weeks. The viruses were then extracted and purified according to established protocols.[30] Select uniformly grown *Nicotiana glutinosa* (*N. glutinosa*) plants at the 5–**7** leaf stage. The half-leaf local lesion assay[31] was employed to evaluate the antiviral activity of the target compounds in terms of curative, protective, and inactivating effects, with cinnamic acid, ningnanmycin, and ribavirin serving as positive controls. All compound solutions, including that of **A23**, were prepared using dimethyl sulfoxide (DMSO) as the primary solvent, followed by dilution as required. Detailed experimental procedures are shown in the Supporting Information 1. Meanwhile, the 50% effective concentration (EC_{50}) values of the compounds were subsequently determined. All measurements were performed in triplicate.

2.4 Molecule docking analysis

The crystal structure of Tobacco Mosaic Virus coat protein (TMV-CP; PDB ID: 1EI7) was obtained from the RCSB Protein Database (www.rcsb.org).[32,33] Small molecule **A23** was constructed using Chem3D 20.0 software and optimized for minimal energy through MM2 molecular mechanics. The complex was prepared in PyMOL 2.4 by removing ligands and redundant water molecules and adding polar and nonpolar hydrogens. Ligand (compound **A23**) and receptor (TMV coat protein, TMV-CP) were subsequently processed with AutoDock Tools 1.5.6 for binding mode prediction. Conformations with the lowest docking scores were selected for analysis, and the docking results were visualized using PyMOL 2.4 software.

2.5 TMV-GFP visualization and systematic infection

The green fluorescent protein-tagged TMV (TMV-GFP) serves as a powerful tool for real-time tracking of systemic viral movement in plants due to its stable fluorescence signature. The progression of systemic infection can be quantitatively assessed by measuring GFP fluorescence intensity and distribution patterns in systemic leaves.[34] To further investigate the antiviral effect of the compound **A23**, the systemic dissemination of TMV-GFP in *Nicotiana benthamiana* (*N. benthamiana*) was monitored. Briefly, when *N. benthamiana* reached the 5–7 leaf stage, they were foliar-sprayed with 500 μg/mL of the test compounds (**A23**, ribavirin, NNM) or a DMSO control. After cultivation for 24 h, TMV-GFP was inoculated onto the lower leaves of each plant. Systemic viral movement was evaluated by visualizing UV-induced GFP fluorescence in newly emerged apical leaves at 7, 10, and 12 days post-inoculation (dpi).

2.6 Evaluation of defense enzyme activity

When *N. benthamiana* plants reached the 5–7 leaf stage, they were sprayed with a 500 μg/mL solution of compound **A23**, with solutions of NNM and DMSO at the same concentration serving as positive and negative controls, respectively. Following a 24 h period, the treated leaves were uniformly dusted with the silicon carbide and subsequently lightly rubbed with a brush that had been carefully dipped into the TMV solution. The plants were then transferred to a growth chamber at 28 ± 1 °C, 10000 Lux light intensity, a 16 h/8 h light/dark cycle, and 75% relative humidity. Afterward, leaf samples were collected at 1, 3, 5, and 7 days post-treatment, immediately flash-frozen in liquid nitrogen, and stored at −80 °C until analysis. The activities of the superoxide dismutase (SOD), phenylalanine ammonia-lyase (PAL), peroxidase (POD) and polyphenol oxidase (PPO) were determined using enzyme assay kits in accordance with the manufacturer's instructions (Suzhou Keming Bioengineering Institute, China). All of the defense enzyme activity tests were repeated three times.

2.7 Chlorophyll content test

The chlorophyll content was extracted and determined using the commercial assay kits (Suzhou Keming Bioengineering Institute, China) following the manufacturer's protocol. Absorbance measurements at 663 and 645 nm were recorded to calculate chlorophyll a, chlorophyll b, and total chlorophyll concentrations according to established equations.[35] All analyses were conducted with three biological replicates.

2.8 Transcriptomics analysis

N. benthamiana plants treated with 500 μg/mL **A23** (**A23** + TMV) and solvent only (CK + TMV) were inoculated with TMV. After 7 days, leaves from the CK + TMV and **A23** + TMV groups were collected. RNA purification, reverse transcription, library construction and sequencing were performed at Shanghai Majorbio Biopharm Biotechnology Co., Ltd. (Shanghai, China) according to the manufacturer's instructions. To identify differentially expressed genes (DEGs) between two different samples, the expression level of each transcript was calculated according to the transcripts per million (TPM) method. DEGs with $|\log_2 FC| \geq 1$ and FDR < 0.05 (determined by DESeq2) were considered to be significantly expressed genes. Differential expression analysis and functional enrichment were performed. In addition, Gene Ontology (GO) functional enrichment and Kyoto Encyclopedia of Genes and Genomes (KEGG) pathway analysis were carried out by Goatools and Python Scipy software, respectively.

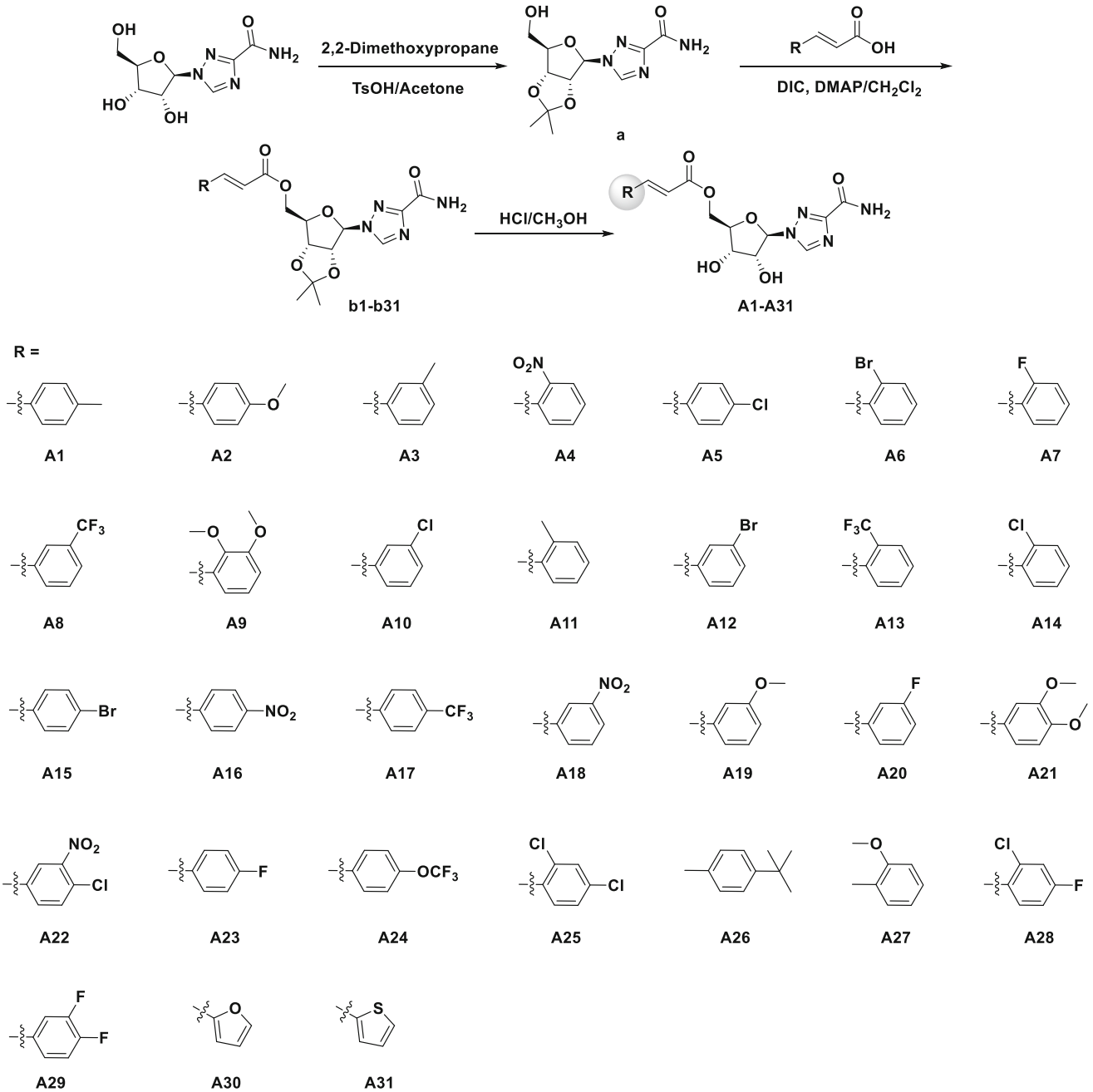

Figure 2. Synthesis routes of compounds **A1 — A31**.

2.9 Salicylic acid content test

N. benthamiana plants were used as the experimental material to assess SA content in three treatment groups: CK, CK + TMV, and **A23** + TMV. SA content was measured using a plant SA ELISA kit (Meimian Industrial Co., Ltd). All experiments were performed with three biological replicates.

2.10 RNA extraction and qRT-PCR validation

N. benthamiana leaves were used to extract the total RNA using Trizol reagent (Changsha CINOTOHI Biotechnology Co., Ltd., China). Reverse transcription was performed using primers and reverse transcriptase kit (Changsha CINOTOHI Biotechnology Co., Ltd., China) per the manufacturer's instructions. Gene expression levels were measured with SYBR Green qPCR mix (Changsha CINOTOHI Biotechnology Co., Ltd., China) on a CFX96 system (BioRad) with a 20 μL reaction volume. All measurements included three biological replicates. The gene expression levels were normalized to actin and calculated relative to controls using the $2^{\Delta\Delta-Ct}$ method.[36]

3 RESULTS AND DISCUSSION

3.1 Chemistry

The synthesis of target compounds was conducted in accordance with the designed synthetic route presented in Fig. 2. In brief, ribavirin was utilized as the starting material, and its C-5′ hydroxyl group was targeted for derivatization. A series of cinnamic acid derivatives bearing diverse substituents were conjugated at this

site, affording novel ribavirin–cinnamic acid hybrids (**A1–A31**). and their antiviral activities against TMV were evaluated. Their structures were identified by ^{1}H NMR, ^{13}C NMR, ^{19}F NMR and HRMS (Supporting Information 1).

3.2 Antiviral bioassays of target compounds A1–A31

The TMV inhibition activity of target compounds **A1–A31** was evaluated, and the results are summarized in Table 1. The findings indicate that most compounds showed potent anti-TMV activity. At a concentration of 500 μg/mL, compounds **A2**, **A6**, **A17**, **A23** and **A24** demonstrated therapeutic activities of 62.1%, 64.6%, 64.5%, 70.0% and 65.0%, respectively; which were better than those of cinnamic acid (30.5%), ribavirin (44.9%) and ningnanmycin (58.8%). Meanwhile, compounds **A10**, **A11**, **A23** and **A31** showed good protective effect on TMV, with protective activity values of 62.2%, 60.2%, 68.0% and 63.7%, respectively. These values surpassed those of both cinnamic acid (36.8%) and ribavirin (45.3%), and were comparable to that of NNM (62.2%). Regrettably, none of the compounds demonstrated superior inactivating activities against TMV compared to NNM (82.8%).

To identify optimal antiviral candidates, we further determined the half-maximal effective concentrations (EC_{50}) of selected compounds against TMV for both curative and protective activities. As shown in Table 2, compounds **A6**, **A17**, **A23** and **A24** exhibited EC_{50} values of 167.2, 175.1, 153.2 and 197.8 μg/mL, respectively, for curative activity, which were superior to those of ribavirin (778.7 μg/mL) and ningnanmycin (285.6 μg/mL). In terms of protective activity, compounds **A10** and **A31** exhibited EC_{50} values of 264.8 and 231.4 μg/mL, respectively. Compound **A23**, which had good anti-TMV protective activity (EC_{50} = 131.1 μg/mL) and no appreciable phytotoxicity toward tobacco at 500 μg/mL (**Fig. S1**), was selected as the most promising compound to further study the mechanism of action.

Table 1. Antiviral activities of target compounds **A1—A31** against TMV at 500 μg/mL.[a]

Compd.	Curative effect (%)	Protective effect (%)	Inactivating effect (%)
A1	55.7 ± 3.7	41.9 ± 4.6	57.3 ± 1.7
A2	62.1 ± 2.5	48.7 ± 2.8	72.6 ± 4.2
A3	57.7 ± 3.2	35.2 ± 6.7	58.0 ± 1.9
A4	51.5 ± 2.3	44.4 ± 1.9	48.6 ± 5.2
A5	55.6 ± 7.6	47.9 ± 1.6	65.4 ± 4.4
A6	64.6 ± 1.8	49.9 ± 3.2	66.7 ± 4.8
A7	56.0 ± 2.3	48.5 ± 4.7	68.2 ± 5.4
A8	52.4 ± 4.8	24.3 ± 3.1	54.7 ± 1.3
A9	56.3 ± 3.2	32.6 ± 4.5	50.8 ± 2.5
A10	38.7 ± 4.3	62.2 ± 1.2	48.1 ± 3.8
A11	56.8 ± 1.4	60.2 ± 3.9	53.2 ± 5.8
A12	48.2 ± 4.8	35.7 ± 1.0	71.0 ± 5.6
A13	57.2 ± 4.7	49.9 ± 3.5	52.7 ± 4.7
A14	42.4 ± 3.0	58.7 ± 3.9	66.8 ± 5.4
A15	58.0 ± 4.8	53.3 ± 3.0	62.0 ± 1.1
A16	43.9 ± 3.9	54.3 ± 3.7	64.2 ± 3.7
A17	64.5 ± 5.6	39.4 ± 2.9	63.5 ± 4.3
A18	60.5 ± 3.9	45.3 ± 3.2	59.9 ± 1.2
A19	63.3 ± 4.8	45.2 ± 3.8	68.1 ± 0.9
A20	61.3 ± 3.8	51.4 ± 3.5	65.5 ± 2.0
A21	58.3 ± 4.2	37.8 ± 3.9	54.3 ± 3.8
A22	59.9 ± 1.5	50.2 ± 3.8	50.9 ± 3.3
A23	70.0 ± 5.2	68.0 ± 3.7	75.0 ± 3.8
A24	65.0 ± 2.6	39.1 ± 2.5	53.5 ± 1.8
A25	49.5 ± 4.8	48.9 ± 4.0	55.7 ± 2.4
A26	41.3 ± 4.6	51.6 ± 3.8	46.9 ± 5.2
A27	53.3 ± 3.2	22.5 ± 2.0	56.3 ± 3.1
A28	57.9 ± 4.3	31.3 ± 1.9	47.9 ± 3.8
A29	45.4 ± 2.1	54.5 ± 2.2	42.2 ± 0.9
A30	36.7 ± 1.4	57.0 ± 2.6	68.7 ± 5.7
A31	53.3 ± 6.4	63.7 ± 3.7	58.9 ± 6.5
Cinnamic acid[b]	30.5 ± 2.7	36.8 ± 2.4	47.7 ± 3.0
Ribavirin[c]	44.9 ± 3.5	45.3 ± 2.5	57.0 ± 3.5
Ningnanmycin[d]	58.8 ± 5.5	62.2 ± 1.2	82.8 ± 5.2

[a] Average of three replicates. Commercial antiviral agent.
[b] Cinnamic acid.
[c] Ribavirin.
[d] Ningnanmycin as the positive control.

Table 2. EC_{50} of several target compounds against TMV[a]

Activity	Compound	Regression equation	R^2	EC_{50} (μg/mL)	95% CI[b]
Curative activity	**A6**	$y = 1.1265\,x + 2.4955$	0.9749	167.2 ± 3.9	132.3–218.0
	A17	$y = 1.2210\,x + 2.2609$	0.9673	175.1 ± 4.4	141.9–234.7
	A23	$y = 1.0374\,x + 2.7387$	0.9787	153.2 ± 5.2	119.6–202.0
	A24	$y = 1.3985\,x + 1.7887$	0.9764	197.8 ± 4.6	151.3–276.3
	Ribavirin	$y = 0.8993\,x + 2.3998$	0.9571	778.7 ± 6.1	539.3–1315.8
	Ningnanmycin	$y = 1.0811\,x + 2.3450$	0.9919	285.6 ± 4.3	217.4–417.1
Protective activity	**A10**	$y = 1.0274\,x + 2.5107$	0.9821	264.8 ± 4.9	200.6–388.8
	A23	$y = 0.6639\,x + 3.6035$	0.9979	131.1 ± 4.0	88.56–197.1
	A31	$y = 0.9934\,x + 2.6512$	0.9626	231.4 ± 6.5	176.3–331.2
	Ribavirin	$y = 1.5694\,x + 0.7247$	0.9999	529.9 ± 6.3	437.1–671.3
	Ningnanmycin	$y = 1.0686\,x + 2.4405$	0.9915	248.4 ± 5.9	188.6–360.6

[a] Average of three replicates. All results are expressed as mean ± SD.
[b] 95% confidence interval.

3.3 Structure–activity relationships (SARs)

The structure–activity relationship (SAR) reveals that the antiviral activity of these compounds depends critically on the electronic character and positional orientation of substituents on the phenyl ring. Moreover, each type of activity (curative, protective, and inactivating) is dictated by distinct structural preferences. Curative activity is markedly enhanced by mono-substitution at the *para*-position, as demonstrated by the efficacy trend **A2** (4-OCH_3) > **A1** (4-CH_3) > **A26** (4-$C(CH_3)_3$), indicating that strong electron-donating groups with hydrogen-bonding capacity (e.g., methoxy) enhance binding affinity, while bulky groups such as *tert*-butyl introduce steric constraints that reduce activity.[37,38] Additionally, the activity also varies when the same substituent is positioned at different locations on the benzene ring. For example, activity gradually increases as fluorine atom shift from the *ortho*- to *meta*- and *para*- positions: **A23** (4-F) > **A20** (3-F) > **A7** (2-F). In contrast, multiple substitutions—exemplified by dimethoxy groups—generally reduce curative efficacy, as seen in the trend **A2** (4-OCH_3) > **A21** (3,4-di-OCH_3) > **A9** (2,3-di-OCH_3), which is likely attributable to increased steric hindrance impairing optimal target engagement.[38] Protective activity, however, is preferentially conferred by heteroaromatic substitutions. The thiophen-2-yl derivative (**A31**) exhibits protective activity comparable to the positive control ningnanmycin and is more effective than the furan-containing analog (**A30**). This effect may be ascribed to thiophene's stronger electron-withdrawing character and higher lipophilicity, which could promote membrane permeability or interactions with hydrophobic regions of the viral coat protein.[39] Certain *meta*- and *ortho*-halogen substitutions, including **A10** (3-Cl) and **A14** (2-Cl), also impart good protective effects. By contrast, strongly electron-withdrawing groups such as NO_2 and CF_3 are generally detrimental, likely due to reduced electron density disrupting effective binding to the viral target.[40] Inactivating activity is optimized by polar substituents at the *para*- or *meta*-positions, as demonstrated by the high efficacy of **A23** (4-F) and **A2** (4-OCH_3), along with *meta*-substituted analogs such as **A12** (3-Br) and **A19** (3-OCH_3). Conversely, *ortho*-substitutions or strongly electron-withdrawing nitro groups consistently diminish virucidal activity.

These findings offer critical structural guidance for designing highly active derivatives. First, multi-targeting agents can be developed by introducing *para*-fluoro or *para*-methoxy groups, which enhance curative and inactivating activities, along with a thiophene ring to improve protective efficacy. Second, substituents should preferentially occupy the *para*- and *meta*-positions, while *ortho*-substitutions, bulky alkyl groups, and strongly electron-withdrawing nitro groups should be avoided to prevent steric and electronic mismatches. Finally, systematic exploration of bioisosteric replacements can help fine-tune lipophilicity and hydrogen-bonding capacity, thereby optimizing both bioavailability and target engagement.

3.4 Molecular docking

The Tobacco Mosaic Virus coat protein (TMV-CP) is critical for viral transcription, translation, elongation, and self-assembly, making it a promising target for anti-TMV agent discovery. We modeled the interaction between compound **A23** and TMV-CP by molecular docking using AutoDock Tools 1.5.6 (Fig. 3). Docking results revealed that the amide oxygen of **A23** forms a hydrogen bond with the backbone N—H of SER138 (3.2 Å). Additionally, the amide N—H and ribose O—H groups formed hydrogen bonds with LEU132 (2.7 Å) and PRO20 (2.3 Å), respectively. The ligand also exhibited a π-alkyl interaction with ILE24, and the fluorine atom on its phenyl ring formed a halogen bond with ASP19. The computed binding energy for the complex was −7.1 kcal/mol, indicating strong binding affinity.

3.5 TMV-GFP visualization and systematic infection

The lower leaves of *N. benthamiana* plants were mechanically inoculated with TMV-GFP, a genetically engineered viral construct created through precise insertion of the GFP reporter gene into the TMV genome. This molecular tagging strategy enables non-invasive, real-time monitoring of viral spread and distribution patterns, as systemic GFP expression in infected tissues generates distinct fluorescence under UV excitation. The green fluorescence of TMV-GFP confirmed that TMV-GFP treated with DMSO successfully replicated and systemically spread from inoculated leaves to newly emerged leaves throughout *N. benthamiana* plants by 7 dpi. After 7 and 12 dpi, the fluorescence intensity in newly emerged leaves continued to intensify, indicating enhanced viral replication and spread. TMV-GFP treated with ribavirin also spread efficiently to newly emerged leaves, exhibiting fluorescence intensity comparable to that in the DMSO treatment from day 7 to day 12. In contrast, **A23** treatment significantly delayed the

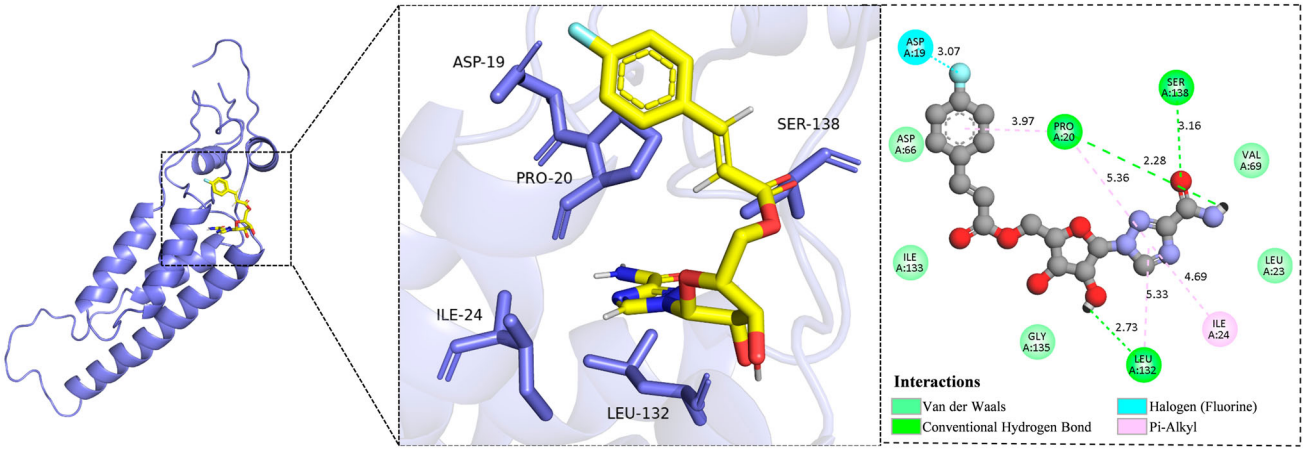

Figure 3. Molecule docking results of compound **A23**.

spread of TMV-GFP, with faint fluorescence signals becoming detectable only at 10 days post-inoculation (Fig. 4). Notably, both the distribution and intensity of fluorescent foci were markedly reduced compared to those in the ribavirin- and NNM-treated control groups. These findings preliminarily indicate that compound **A23** can inhibit the proliferation and long-distance movement of TMV.

3.6 Defensive enzyme activity assessment

Some major defense enzymes, such as superoxide dismutase (SOD), phenylalanine ammonia-lyase (PAL), peroxidase (POD) and polyphenol oxidase (PPO), can significantly enhance the plant's own defense activity and induce plant disease resistance.[41] The bioactivities of the defensive enzymes in tobacco leaves were evaluated using the antiviral agents of NNM and **A23**. The TMV solution was applied to the tobacco leaves after 24 h post-treatment with antiviral agents. As depicted in Fig. 5, the target compound **A23** can enhance the activity of SOD, PAL, POD and PPO in tobacco. SOD, as an important metal antioxidant enzyme in living organisms, can catalyze the disproportionation reaction of superoxide anion (O^{2-}) to generate hydrogen peroxide (H_2O_2) and oxygen (O_2). Its activity level can be used as an important indicator for evaluating the stress resistance of plants.[42] As shown in Fig. 5(A), in the **A23** + TMV treatment group, SOD activity increased gradually during the first 3 days and peaked on day 3. Subsequently, it declined slowly from day 3 to day 7. Throughout the trial, the SOD activity in the **A23** + TMV group was consistently higher than that in both the CK + TMV and NNM + TMV groups, with the exception of day 1, on which it measured slightly lower than in the NNM + TMV group. On the fifth day, the activity

Figure 4. TMV-GFP fluorescence observed under UV-365 nm excitation in *N. benthamiana* after pretreatment with compounds for 7, 10, and 12 days. (green fluorescence represents visible TMV-GFP in leaves and red represents no TMV-GFP in part of leaves).

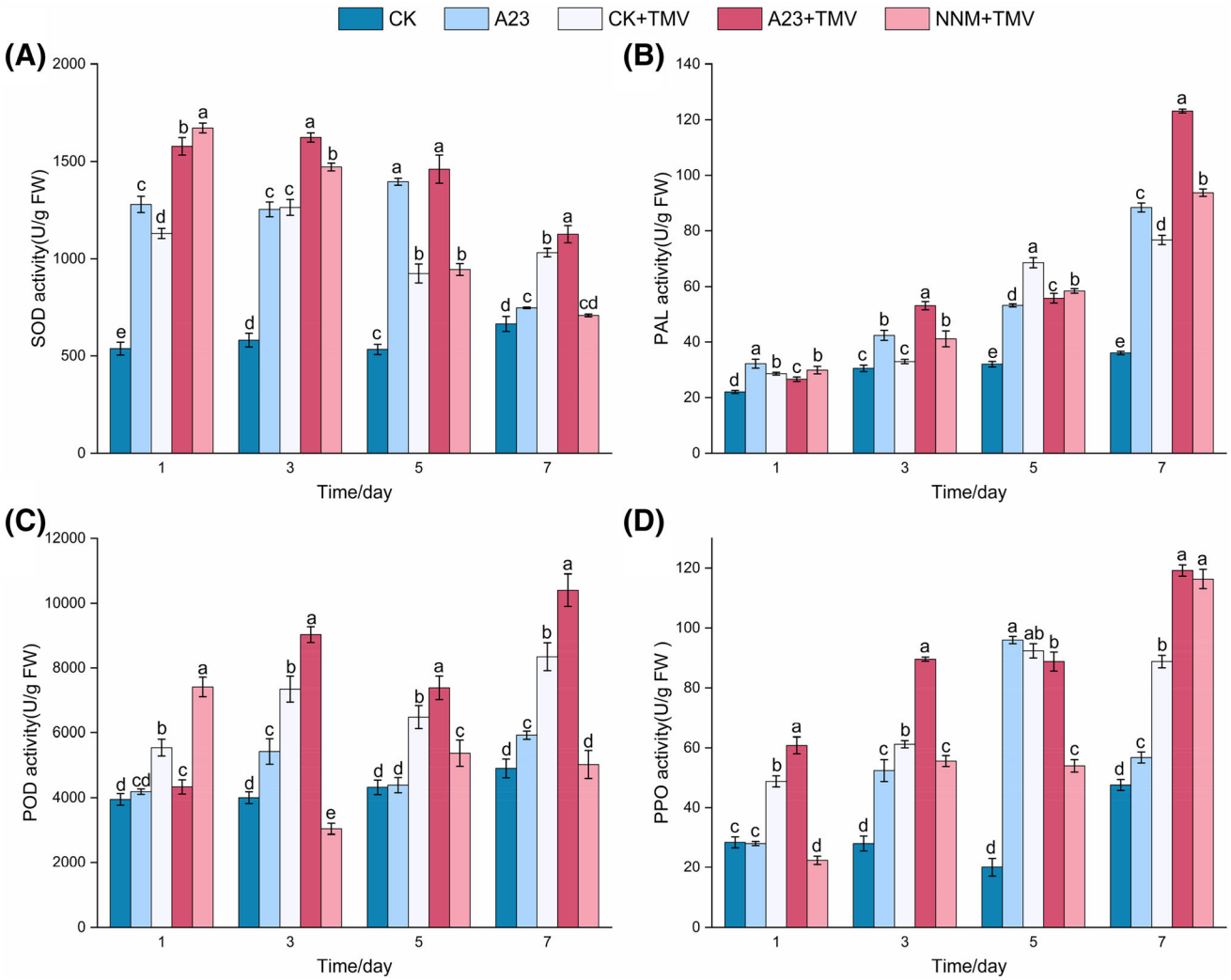

Figure 5. Effect of compound **A23** on defense enzymes from tobacco. (A) SOD. (B) PAL. (C) POD. (D) PPO. Straight bars signify the means and standard deviation of three independent experiments. Lowercase letters indicate significant differences among different treatment groups, as determined by one-way analysis of variance (ANOVA; $P < 0.05$).

was 1.6-fold and 1.6-fold higher than those of the CK + TMV and NNM + TMV groups, respectively.

PAL activates the system to acquire resistance by inducing the biosynthetic pathways of secondary metabolites such as lignin and phytochemicals, strengthens the cell wall and inhibits pathogen infection.[43] As shown in Fig. 5(B), in the compound **A23** treatment group, PAL activity rose gradually during days 1 to day 5, then increased sharply from day 5 to day 7. On the seventh day after TMV inoculation, the PAL activity in the **A23** + TMV group was 1.6-fold and 1.3-fold higher than those of the CK + TMV and NNM + TMV groups, respectively.

POD is a crucial defense-related enzyme in plants. It can scavenge excess hydrogen peroxide (H_2O_2) and oxygen free radicals, thereby mitigating oxidative stress. Furthermore, this enzyme actively participates in lignin biosynthesis by catalyzing the polymerization of monolignols, which promotes lignification. The enhanced lignification strengthens plant cell walls, contributing significantly to improved disease resistance mechanisms.[44] As illustrated in Fig. 5(C), although the POD activity in the **A23** + TMV treatment group was lower than in both the CK + TMV and NNM + TMV groups on day 1, it surpassed those of all control groups from day 3. The activity peaked on day 7, with values reaching 1.3-fold and 2.1-fold higher than those in the CK + TMV and NNM + TMV groups, respectively.

PPO is a copper-containing oxidoreductase that catalyzes the formation of quinone substances from phenolic substances during the growth and development of crops, thereby enhancing resistance against diseases and pests.[45] Fig. 5(D) demonstrates that the **A23** + TMV treatment group induced a progressive enhancement in PPO activity, paralleling the increasing pattern of PAL activity. On the third day, the activity levels were 1.5-fold and 1.6-fold higher than those in the CK + TMV group and NNM + TMV treatment group, respectively. On the seventh day, the PPO activity was 1.3-fold higher than that in the CK + TMV group and slightly higher than that in the NNM + TMV group.

In summary, the evaluation of defense enzyme activities indicates that the compound **A23** enhances the activities of PAL, SOD, POD, and PPO, thereby improving plant disease resistance. It is postulated that the pronounced efficacy of **A23** in activating these defense enzymes significantly contributes to its high protective activity against TMV.

3.7 Chlorophyll content test

Chlorophyll is a crucial component of chloroplasts and plays a vital role in photosynthesis. In this study, the contents of chlorophyll a, chlorophyll b, and total chlorophyll were measured. Figure 6 shows the changes in chlorophyll content for each experimental group on days 1, 3, 5, and 7 after viral inoculation. The results indicate that compound **A23** significantly altered the chlorophyll a, chlorophyll b, and total chlorophyll levels in tobacco leaves. On the first day, the **A23** + TMV treatment group exhibited significantly higher chlorophyll content compared to both the CK group and the CK + TMV group. Specifically, the chlorophyll a, chlorophyll b, and total chlorophyll levels in the **A23** + TMV group reached 2.2-fold, 3.2-fold, and 2.4-fold those of the CK group, and 3.0-fold, 3.1-fold, and 3.1-fold those of the CK + TMV group, respectively. Furthermore, the chlorophyll content (including chlorophyll a, b, and total chlorophyll) of the **A23** + TMV treatment group showed a progressive increase from day 1 to day 7 post-treatment. On day 7, this group showed significantly higher chlorophyll levels than both the CK and CK + TMV groups. The chlorophyll a, b, and total chlorophyll values reached 1.5-fold, 2.2-fold, and 1.6-fold those of the CK group, respectively. Compared to the CK + TMV group, the values were 1.5-fold, 1.4-fold, and 1.5-fold higher, while also exceeding the NNM + TMV treatment group by 1.2-fold, 1.1-fold, and 1.1-fold, respectively. Therefore, we hypothesize that compound **A23** can stimulate the immune system of tobacco plants by increasing the content of chlorophyll in the plants, promoting photosynthesis and thereby improve disease resistance.

3.8 Transcriptomic analysis

To clarify the regulatory effect of **A23** on gene expression, signaling pathways, and host responses, RNA sequencing was executed to identify the key DEGs in TMV-inoculated *N. benthamiana* following control or 500 μg/mL **A23** treatment. A total of 27 577 genes (TPM > 1) were identified, with 25 985 genes identified in the CK + TMV group (including 2132 specifically expressed genes)

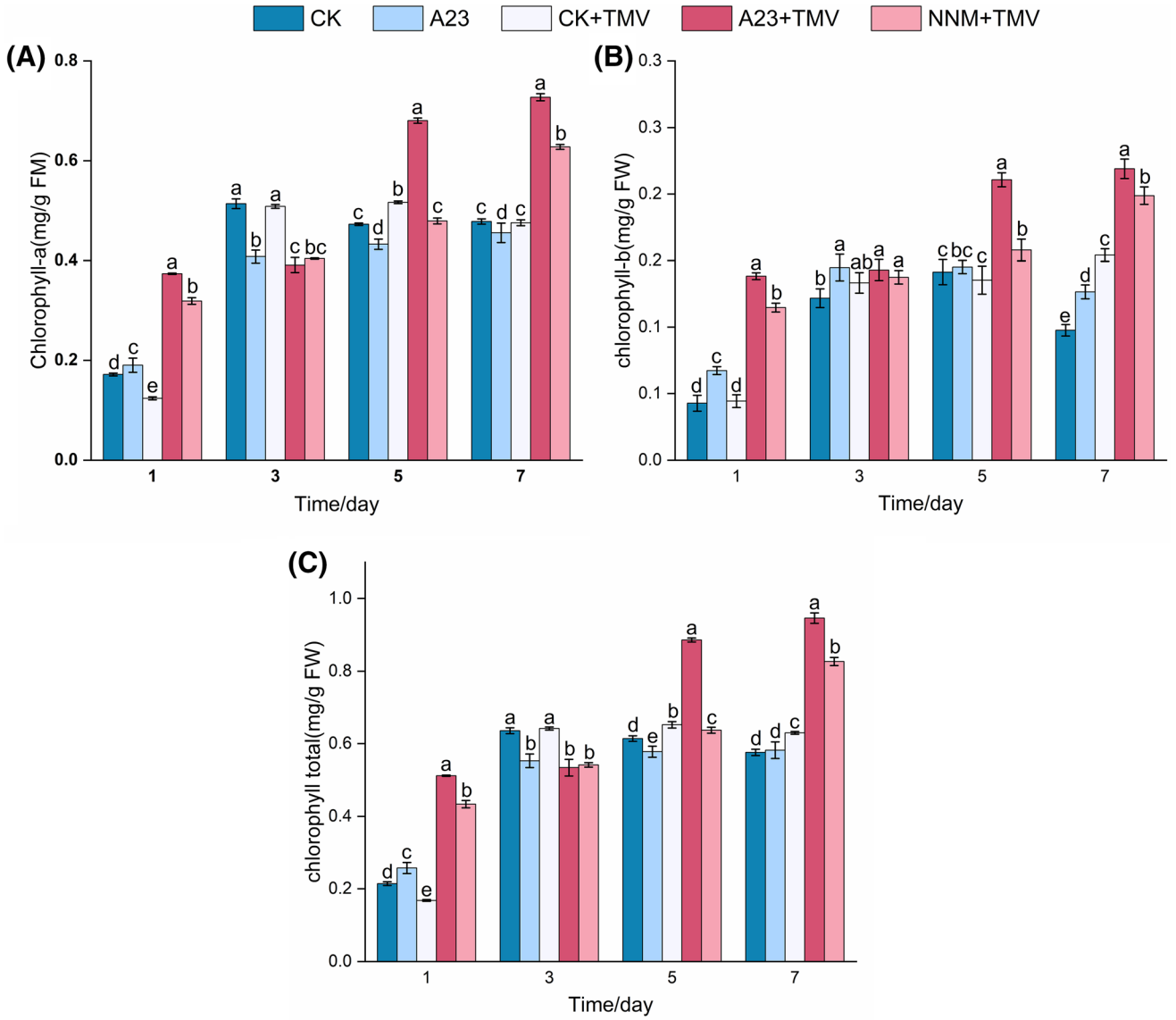

Figure 6. Effect of compound **A23** on chlorophyll content from tobacco leaves. (A) Chlorophyll a. (B) Chlorophyll b. (C) Total chlorophyll content. Straight bars signify the means and standard deviation of three independent experiments. Lowercase letters indicate significant differences among different treatment groups, as determined by one-way analysis of variance (ANOVA; $P < 0.05$).

and 25 445 genes in the **A23** + TMV group (including 1592 specifically expressed genes) (Fig. 7(A) and Table S1). Of the total DEGs identified in the CK + TMV and **A23 +** TMV groups, 4512 genes were downregulated and 5321 genes were upregulated. (Fig. 7 (B) and Table S1).

GO term enrichment analysis ($P < 0.05$) of DEGs of the CK + TMV and **A23** + TMV groups is shown in Fig. 7(C) and Table S2. In BP categories, DEGs were predominantly enriched in processes such as cellular process, biological regulation and response to stimulus. Within the MF, enrichment was observed for binding, catalytic activity and transporter activity. In CC, membrane showed significant enrichment. To study the mechanism of action induced by A23, a functional pathway analysis was performed using the KEGG database. As shown in Fig. 7(D) and Table S3, the main enriched pathways for the differential genes included plant hormone signal transduction (ko04075, 190 DEGs), plant-pathogen interaction (ko00620, 116 DEGs), MAPK signaling pathway (ko04016, 84 DEGs), starch and sucrose metabolism (ko01187, 80 DEGs) and amino sugar and nucleotide sugar metabolism (ko00966, 75 DEGs).

A total of 190 DEGs were enriched (105 upregulated, 85 downregulated) on the plant hormone signal transduction pathway. These genes function in multiple phytohormone pathways—including auxin, cytokinin, abscisic acid, ethylene, brassinosteroid, jasmonic acid, and SA—and are linked to development, defense, and stress adaptation.[46] Phytohormones act as central regulators of plant immunity, coordinating defense responses while maintaining growth-defense balance.[47] *NPR1* is an indispensable positive regulator in the process of salicylic acid (SA)-mediated systemic acquired resistance (SAR) in plants. Overexpression of *NPR1* in a wide range of plant species, including many crops, has been shown to enhance disease resistance against various pathogens and abiotic stresses. In the SA signal transduction pathway, pathogenesis-related protein 1 (*PR-1*) is widely recognized as a critical defense marker protein during plant responses to biotic and abiotic stresses.[48] Its transcriptional activation is a core molecular event in the establishment of SAR, and therefore, the overexpression of *PR-1* is commonly used as a reliable marker for SA-mediated defense responses.[49] In this study, **A23** + TMV treatment significantly upregulated *NPR1*, *TGA* transcription factors, and *PR-1* compared to the control, indicating that **A23** treatment successfully activates the SA signaling pathway, thereby enhancing the systemic defense capacity of *N. benthamiana* against TMV. Furthermore, **A23** treatment differentially regulates a range of phytohormone-responsive genes, including auxin-binding or responsive genes (*SAUR32*, *IAA17*, *IAA20D* and *ARF4*), *ethylene-responsive transcription factor ERF1*, pathogenesis-related protein 1 (*PR-1*), ABA receptor genes and serine/threonine-protein kinase *SnPK2*. Therefore, we propose that **A23** modulates complex signaling networks and coordinate multiple hormone pathways to confer resistance against viral invasion.

Our results also indicate that **A23** differentially modulates the expression of various defense-related genes. Pattern-triggered immunity (PTI) serves as an evolutionarily conserved foundation of plant innate immunity, initiated when pattern recognition receptors (PRRs) perceive pathogen-associated molecular patterns (PAMPs).[50,51] This recognition rapidly activates downstream immune responses—such as ethylene biosynthesis, reactive oxygen species (ROS) accumulation, and callose deposition—to inhibit pathogen invasion.[52] Conversely, effector-triggered immunity (ETI) is triggered upon detection of pathogen effectors by intracellular resistance proteins, leading to salicylic acid (SA) synthesis and systemic acquired resistance (SAR). PTI and ETI reinforce each other to produce more robust plant defense responses against pathogen infections.[53] In this study, the expression of genes in the heat shock protein (Hsp) family, including

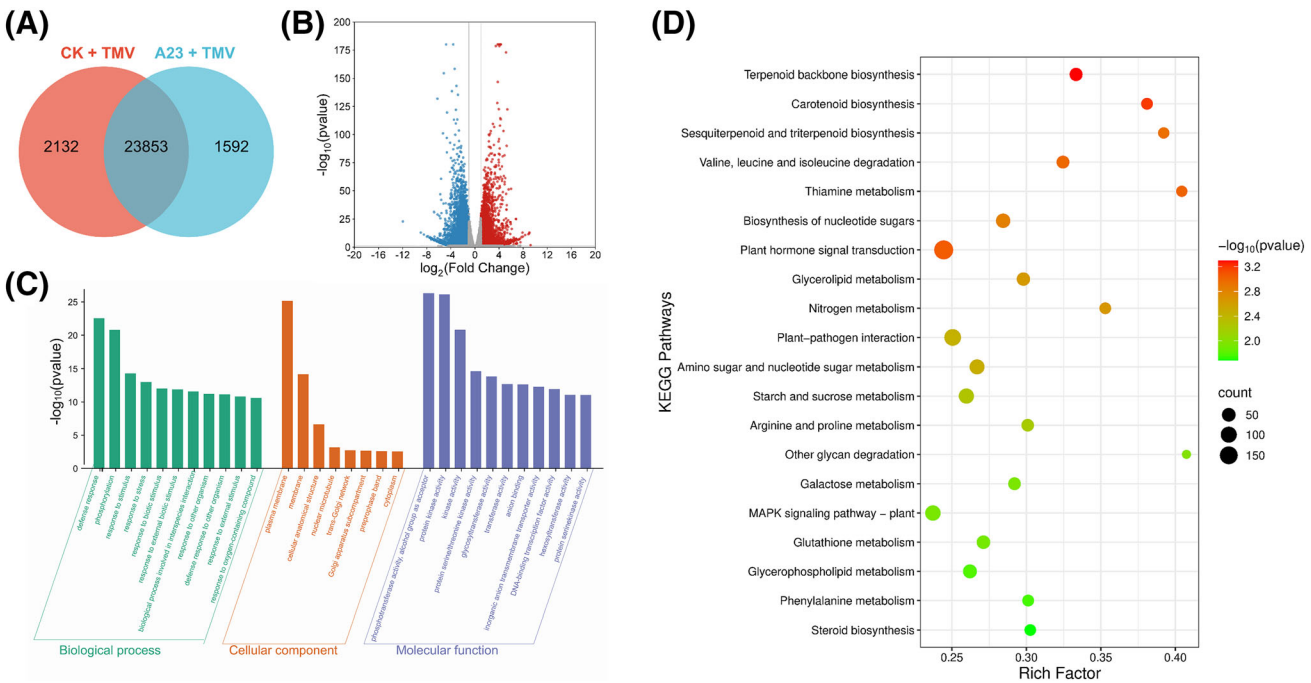

Figure 7. Analysis of the DEGs between **A23** + TMV and CK + TMV treatments. (A) Venn diagram and (B) Volcano plot for genes identified. Red dots represent upregulated DEGs, blue dots represent down-expressed DEGs, and gray dots represent non-DEGs. (C) Enriched GO terms of DEGs ($P < 0.05$). (D) Enriched KEGG pathway of DEGs ($P < 0.05$).

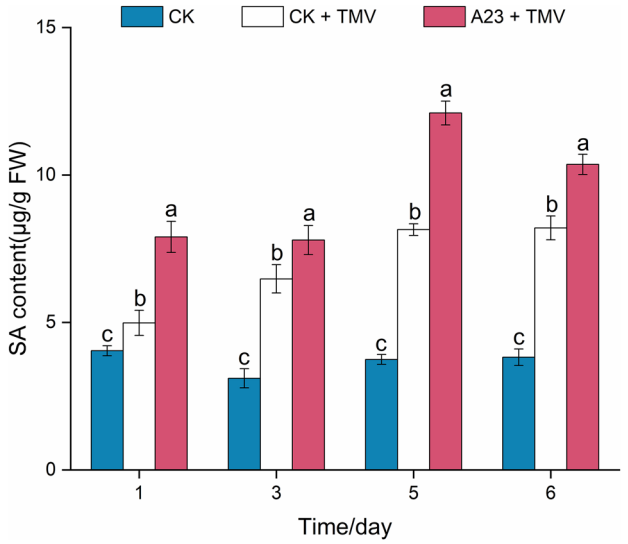

Figure 8. Effect of compound **A23** on salicylic acid (SA) content in *N. benthamiana*. Straight bars signify the means and standard deviation of three independent experiments. Lowercase letters indicate significant differences among different treatment groups, as determined by one-way analysis of variance (ANOVA; $P < 0.05$).

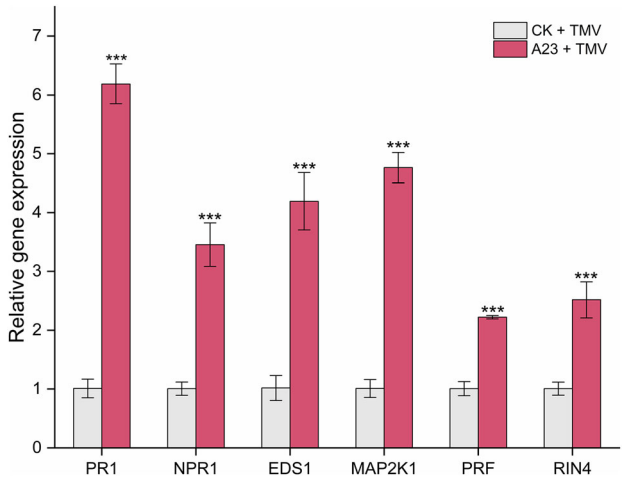

Figure 9. Validation of transcriptomic data by qRT-PCR for six upregulated DEGs. Values are mean ± SD (n = 3). $^{*}P < 0.05$, $^{**}P < 0.01$, $^{***}P < 0.001$.

Hsp90A and *Hsp90B*, was significantly induced. Similarly, our results showed that **A23** induced a significant upregulation of *FLS2*, the disease resistance protein *PRF*, the enhanced disease susceptibility 1 protein *EDS1* and the RPM1-interacting protein 4 (*RIN4*). Collectively, the upregulation of these genes in response to **A23** treatment likely inhibited TMV multiplication by activating plant innate immune responses, including both PTI and ETI.

3.9 SA content analysis

SA is a key phytohormone essential for plant resistance to pathogens, and its accumulation triggers the SA signaling pathway.[54] To obtain a more comprehensive understanding of the influence of **A23** on SA signaling, we quantified SA levels in *N. benthamiana* in three treatment groups: CK, CK + TMV, and **A23** + TMV. The results showed that SA content in the **A23** + TMV group increased gradually over time, peaking on day 5 at a level 1.5-fold higher than that in the CK + TMV group. Despite a slight decrease by day 7, the SA level was still 1.3-fold higher than that in the CK + TMV group (Fig. 8). These results suggest that compound **A23** enhances viral disease resistance by promoting SA accumulation and subsequent activation of the SA signaling transduction pathway.

3.10 qRT-PCR validation

To validate the accuracy of the Illumina sequencing results, we selected six genes (*PR1*, *NPR1*, *EDS1*, *MAP2K1*, *PRF*, and *RIN4*) for qRT-PCR analysis on day 7 after treatment with compound **A23**. The primer sequences are listed in Table S4, and the results are shown in Fig. 9. The qRT-PCR results were consistent with the sequencing data, thus confirming the reliability of our transcriptomic analysis.

4 CONCLUSION

In conclusion, a series of cinnamic acid-conjugated ribavirin derivatives were successfully synthesized and systematically evaluated for their anti-TMV activity. Most of the synthesized compounds exhibited notable antiviral properties in bioassays. Notably, compound **A23** demonstrated the most potent protective activity against TMV, with an EC_{50} value of 131.1 μg/mL, which was superior to the commercial agent ningnanmycin (248.4 μg/mL). In addition, **A23** effectively inhibited the systemic infection of TMV-GFP in *N. benthamiana*, as subsequently confirmed through visualization. Further studies on defense enzyme activity indicated that **A23** increased the activities of PAL, SOD, POD and PPO, thereby enhancing plant resistance to diseases. Transcriptomic analysis revealed that **A23** enhances antiviral resistance in plants through the coordinated regulation of a complex signaling network, which integrates multiple hormonal pathways and includes the specific activation of salicylic acid-mediated signaling. Therefore, **A23** represents a promising candidate for development as both an antiviral agrochemical and a plant resistance inducer capable of effectively suppressing TMV infection while activating the plant immune system to establish acquired resistance.

ACKNOWLEDGEMENTS

We acknowledge financial support from the National Natural Science Fund for Excellent Young Scientists Fund Program (Overseas); the starting grant of Guizhou University [(2024) 01]; National Natural Science Foundation of China (U23A20201, 32502555); Singapore National Research Foundation under its NRF Competitive Research Program (NRF-CRP22-2019-0002); Ministry of Education, Singapore, under its MOE AcRF Tier 1 Award (RG84/22, RG70/21), MOE AcRF Tier 2 (MOE-T2EP10222-0006); a Chair Professorship Grant, and Nanyang Technological University; National Key Research and Development Program of China (2022YFD1700300), the Program of Introducing Talents of Discipline to Universities of China (111 Program, D20023) at Guizhou University, the Central Government Guides Local Science and Technology Development Fund Projects [Qiankehezhongyindi (2024) 007, (2023)001].

DATA AVAILABILITY STATEMENT

The data that supports the findings of this study are available in the supplementary material of this article.

CONFLICT OF INTEREST

The authors declare no competing financial interest.

SUPPORTING INFORMATION

Supporting information may be found in the online version of this article.

REFERENCES

1 An MN, Zhao XX, Zhou T, Wang GZ, Xia ZH and Wu YH, A novel biological agent cytosinpeptidemycin inhibited the pathogenesis of tobacco mosaic virus by inducing host resistance and stress response. *J Agric Food Chem* **27**:7738–7747 (2019).
2 Yan CC, Dong JY, Liu YX, Li YQ and Wang QM, Target-directed design, synthesis, antiviral activity, and SARs of 9-substituted phenanthroindolizidine alkaloid derivatives. *J Agric Food Chem* **27**:7565–7571 (2021).
3 Sun W, Liao AJ, Lei L, Tang X, Wang Y and Wu J, Research progress on piperidine-containing compounds as agrochemicals. *Chin Chem Lett* **1**:109855 (2025).
4 Liao AJ, Sun W, Liu YM, Yan H, Xia Z and Wu J, Pyrrole and pyrrolidine analogs: the promising scaffold in discovery of pesticides. *Chin Chem Lett* **3**:110094 (2025).
5 Wang Y, Guo SS, Sun W, Tu H, Tang Y, Xu Y *et al.*, Synthesis of 4H-pyrazolo [3, 4-*d*] pyrimidin-4-one hydrazine derivatives as a potential inhibitor for the self-assmbly of TMV particles. *J Agric Food Chem* **6**:2879–2887 (2024).
6 Jones RAC and Naidu RA, Global dimensions of plant virus diseases: current status and future perspectives. *Annu Rev Virol* **1**:387–409 (2019).
7 Adeel M, Farooq T, White JC, Hao Y, He Z and Rui Y, Carbon-based nanomaterials suppress tobacco mosaic virus (TMV) infection and induce resistance in *Nicotiana benthamiana*. *J Hazard Mater* **404**: 124167 (2021).
8 Gan XH, Hu DY, Li P, Wu J, Chen XW, Xue W *et al.*, Design, synthesis, antiviral activity and three-dimensional quantitative structure activity relationship study of novel 1,4-pentadien-3-one derivatives containing the 1,3,4-oxadiazole moiety. *Pest Manag Sci* **3**:534–543 (2016).
9 Wang ZW, Wei P, Liu YX and Wang QM, D and E rings may not be indispensable for antofine: discovery of phenanthrene and alkylamin chain containing antofine derivatives as novel antiviral agents against tobacco mosaic virus (TMV) based on interaction of antofine and TMV RNA. *J Agric Food Chem* **43**:10393–10404 (2014).
10 Su B, Cai C, Deng M and Wang QM, Spatial configuration and 3D conformation directed design, synthesis, antiviral activity, and structure-activity relationships (SARs) of phenanthroindolizidine analogues. *J Agric Food Chem* **10**:2039–2045 (2016).
11 Jordheim LP, Durantel D, Zoulim F and Dumontet C, Advances in the development of nucleoside and nucleotide analogues for cancer and viral diseases. *Nat Rev Drug Discov* **6**:447–464 (2013).
12 Pawlotsky JM, Dahari H, Neumann AU, Hezode C, Germanidis G, Lonjon I *et al.*, Antiviral action of ribavirin in chronic hepatitis C. *Gastroenterology* **3**:703–714 (2004).
13 Bittner H, Schenk G, Schuster G and Kluge S, Elimination by chemotherapy of potato virus S from potato plants grown in vitro. *Potato Res* **2**: 175–179 (1989).
14 Parker WB, Metabolism and antiviral activity of ribavirin. *Virus Res* **2**: 165–171 (2005).
15 Li J, Cao L, Zhao Y, Shen J, Wang L, Feng M *et al.*, Structural basis for the activation of plant bunyavirus replication machinery and its dual-targeted inhibition by ribavirin. *Nat Plants* **11**:518–530 (2025).
16 Gerwick BC and Sparks TC, Natural products for pest control: an analysis of their role, value and future. *Pest Manag Sci* **8**:1169–1185 (2014).
17 Yuan M, Tian Z, Yin X, Yuan X, Gao J, Yuan W *et al.*, Structural optimization of the natural product: discovery of almazoles C–D and their derivatives as novel antiviral and anti-phytopathogenic fungus agents. *J Agric Food Chem* **50**:15693–15702 (2022).
18 El-Seedi HR, El-Said AM, Khalifa SA, Goransson U, Bohlin L, Borg-Karlson AK *et al.*, Biosynthesis, natural sources, dietary intake, pharmacokinetic properties, and biological activities of hydroxycinnamic acids. *J Agric Food Chem* **44**:10877–10895 (2012).
19 Tani H, Hikami S, Takahashi S, Kimura Y, Matsuura N, Nakamura T *et al.*, Isolation, identification, and synthesis of a new prenylated cinnamic acid derivative from Brazilian green propolis and simultaneous quantification of bioactive components by LC-MS/MS. *J Agric Food Chem* **44**:12303–12312 (2019).
20 Zhou K, Chen DD, Li B, Zhang BY, Miao F and Zhou L, Bioactivity and structure–activity relationship of cinnamic acid esters and their derivatives as potential antifungal agents for plant protection. *PLoS One* **4**:e0176189 (2017).
21 Wang YL, Niu S, Yu HT, Yang GZ, Liu YQ, Hu G *et al.*, Discovery of acaricidal, insecticidal, and fungicidal candidates inspired by natural ethyl cinnamate compounds isolated from polygonum orientale L. *J Agric Food Chem* **45**:24967–24978 (2024).
22 Wang J, Lou J, Luo C, Zhou L, Wang M and Wang L, Phenolic compounds from Halimodendron halodendron (pall.) Voss and their antimicrobial and antioxidant activities. *Int J Mol Sci* **9**:11349–11364 (2012).
23 Buxton T, Takahashi S, Eddy-Doh AM, Baffoe-Ansah J, Owusu EO and Kim CS, Insecticidal activities of cinnamic acid esters isolated from *Ocimum gratissimum* L. and *Vitellaria paradoxa* Gaertn leaves against *Tribolium castaneum* Hebst (Coleoptera: Tenebrionidae). *Pest Manag Sci* **1**:257–267 (2020).
24 Vishnoi S, Agrawal V and Kasana VK, Synthesis and structure–activity relationships of substituted cinnamic acids and amide analogues: a new class of herbicides. *J Agric Food Chem* **8**:3261–3265 (2009).
25 Wu ZX, Zhang J, Chen JX, Pan JK, Zhao L, Liu DY *et al.*, Design, synthesis, antiviral bioactivity and three-dimensional quantitative structure-activity relationship study of novel ferulic acid ester derivatives containing quinazoline moiety. *Pest Manag Sci* **10**:2079–2089 (2017).
26 Gan XH, Hu DY, Wang YJ, Yu L and Song BA, Novel trans-ferulic acid derivatives containing a chalcone moiety as potential activator for plant resistance induction. *J Agric Food Chem* **22**:4367–4377 (2017).
27 Wang Y, Song S, Zhang W, Deng Q, Feng Y, Tao M *et al.*, Deciphering phenylalanine-derived salicylic acid biosynthesis in plants. *Nature* **645**:208–217 (2025).
28 Lv J, Zou J, Nong YL, Song J, Shen TW, Cai H *et al.*, Catalytic regioselective acylation of unprotected nucleosides for quick access to COVID and other nucleoside prodrugs. *ACS Catal* **13**:9567–9576 (2023).
29 Zhu J, Li Q, Yu X, Zhang X, Li H, Wen K *et al.*, Synthesis of hapten, production of monoclonal antibody, and development of immunoassay for ribavirin detection in chicken. *J Food Sci* **7**:2851–2860 (2021).
30 Gan XH, Wang ZX and Hu DY, Synthesis of novel antiviral ferulic acid –eugenol and isoeugenol hybrids using various link reactions. *J Agric Food Chem* **46**:13724–13733 (2021).
31 Wu ZX, Zhang J, Chen JX, Pan JK, Zhao L, Liu DY *et al.*, Design, synthesis, antiviral bioactivity and three-dimensional quantitative structure–activity relationship study of novel ferulic acid ester derivatives containing quinazoline moiety. *Pest Manag Sci* **73**:2079–2089 (2017).
32 Xu FZ, Guo SS, Zhang W, Wang YY, Wei PP, Chen SH *et al.*, Trifluoromethylpyridine thiourea derivatives: design, synthesis and inhibition of the self-assembly of tobacco mosaic virus particles. *Pest Manag Sci* **78**:1417–1427 (2022).
33 Cai H, Zhang X, Ling D, Zhang M, Pang C, Chen ZY *et al.*, Discovery of pyridyl-benzothiazol hybrids as novel protoporphyrinogen oxidase inhibitors via scaffold hopping. *J Agric Food Chem* **72**:8963–8972 (2024).
34 Shao WB, Wang PY, Fang ZM, Wang JJ, Guo DX, Ji J *et al.*, Synthesis and biological evaluation of 1,2,4-Triazole thioethers as both potential virulence factor inhibitors against plant bacterial diseases and agricultural antiviral agents against tobacco mosaic virus infections. *J Agric Food Chem* **50**:15108–15122 (2021).
35 Yu L, Guo S, Wang Y, Liao A, Zhang W, Sun P *et al.*, Design, synthesis, and bioactivity of spiro derivatives containing a pyridine moiety. *J Agric Food Chem* **50**:15726–15736 (2022).
36 Livak KJ and Schmittgen TD, Analysis of relative gene expression data using real-time quantitative PCR and the $2^{-\Delta\Delta CT}$ method. *Methods* **25**:402–408 (2001).
37 Zheng Z, Dai AL, Wang Y, Guo SS, Ning F, Yang S *et al.*, Design, enantioselective synthesis, and antiviral activities against tobacco mosaic virus (TMV) of axially chiral Biaryl derivatives. *J Agric Food Chem* **73**: 15514–15523 (2025).
38 Pinheiro PD, Franco LS and Fraga CA, The magic methyl and its tricks in drug discovery and development. *Pharmaceuticals* **16**:1157 (2023).
39 Thakur S, Kumar D, Jaiswal S, Goel KK, Rawat P, Srivastava V *et al.*, Medicinal chemistry-based perspectives on thiophene and its

derivatives: exploring structural insights to discover plausible drug-gable leads. *Pharm Med Sci* **16**:481–510 (2025).
40 Zhong QF, Liu R and Liu G, Structure–activity relationship studies on quinoxalin-2 (1*H*)-one derivatives containing thiazol-2-amine against hepatitis C virus leading to the discovery of BH6870. *Mol Divers* **19**:829–853 (2015).
41 Hanaka A, Wójcik M, Dresler S, Mroczek-Zdyrska M and Maksymiec W, Does methyl jasmonate modify the oxidative stress response in Phaseolus coccineus treated with Cu? *Ecotox Environ Safe* **124**:480–488 (2016).
42 Zhou Y, Sun Z, Zhou Q, Zeng W, Zhang M, Feng S *et al*., Novel flavonol derivatives containing benzoxazole as potential antiviral agents: design, synthesis, and biological evaluation. *Mol Divers* **6**:3919–3935 (2024).
43 Liu J, Lefevere H, Coussement L, Delaere I, De Meyer T, Demeestere K *et al*., The phenylalanine ammonia-lyase inhibitor AIP induces rice defence against the root-knot nematode meloidogyne graminicola. *Mol Plant Pathol* **1**:e13424 (2024).
44 Chen J, Shi J, Yu L, Liu DY, Gan XH, Song BA *et al*., Design, synthesis, antiviral bioactivity, and defense mechanisms of novel dithioacetal derivatives bearing a strobilurin moiety. *J Agric Food Chem* **21**:5335–5345 (2018).
45 Zhang S, Recent advances of polyphenol oxidases in plants. *Molecules* **5**:2158 (2023).
46 Wang CY, Liu Y, Li SS and Han GZ, Insights into the origin and evolution of the plant hormone signaling machinery. *Plant Physiol* **3**:872–886 (2015).
47 Mine A, Seyfferth C, Kracher B, Berens ML, Becker D and Tsuda K, The defense phytohormone signaling network enables rapid, high-amplitude transcriptional reprogramming during effector-triggered immunity. *Plant Cell* **6**:1199–1219 (2018).
48 Kumar P, Pandey S and Pati PK, Interaction between pathogenesis-related (PR) proteins and phytohormone signaling pathways in conferring disease tolerance in plants. *Physiol Plant* **2**:e70174 (2025).
49 Anuradha C, Chandrasekar A, Backiyarani S, Thangavelu R, Giribabu P and Uma S, Genome-wide analysis of pathogenesis-related protein 1 (PR-1) gene family from Musa spp. and its role in defense response during stresses. *Gene* **821**:146334 (2022).
50 Boutrot F and Zipfel C, Function, discovery, and exploitation of plant pattern recognition receptors for broad-spectrum disease resistance. *Annu Rev Phytopathol* **1**:257–286 (2017).
51 Nie J, Zhou W, Liu J, Tan N, Zhou JM and Huang L, A receptor-like protein from *Nicotiana benthamiana* mediates VmE02 PAMP-triggered immunity. *New Phytol* **4**:2260–2272 (2021).
52 Fu ZQ and Dong X, Systemic acquired resistance: turning local infection into global defense. *Annu Rev Plant Biol* **1**:839–863 (2013).
53 Ngou BP, Ahn HK, Ding P and Jones JD, Mutual potentiation of plant immunity by cell-surface and intracellular receptors. *Nature* **592**:110–115 (2021).
54 Zhu F, Li K, Cao M, Zhang Q, Zhou Y, Chen H *et al*., *NbNAC1* enhances plant immunity against TMV by regulating isochorismate synthase 1 expression and the SA pathway. *Plant J* **4**:e17242 (2025).